BBAA VI International Colloquium on:
Bluff Bodies Aerodynamics & Applications
Milano, Italy, July, 20-24 2008

CHARACTERISTIC OF WIND LOAD ON A HEMISPHERICAL DOME IN SMOOTH FLOW AND TUBULENT BOUNDARY LAYER FLOW

C. M. Cheng[*], C. L. Fu[†], Y.Y. Lin[#]

[*] Department of Civil Engineering, Tamkang University
151 Ying-chuan Road Tamsui,Taipei, Taiwan 25137
[*]e-mails: cmcheng@mail.tku.edu.tw, [†] fcl@mail.tku.edu.tw, [#]yyl@mail.tku.edu.tw

Keywords: wind load, hemispherical dome, wind tunnel, smooth flow, turbulent boundary layer, Reynolds number

1 INTRODUCTION

Hemispherical dome has been a common structural geometry shape for large span sports stadium or storage purposes. The curve shape makes the accurate estimation of the wind pressure fluctuations on a hemispherical dome a difficult task due to the Reynolds number effects. In the past, several research articles have been focused on this subject. Among them, Maher[1] reported the drag coefficient becomes invariant when Reynolds number exceeds 1.4×10^6. Taylor[2] suggests that, when Reynolds numbers exceeds 2.0×10^5 and turbulence intensity exceeds 4%, the pressure distribution becomes Reynolds number independent. Ogawa [3] indicates that for Reynolds numbers ranging from 1.2×10^5 ~2.1×10^5, level of turbulence has little effect upon the mean pressure distribution. Toy and Moss [4] show that with increase of turbulence intensity, separation region and reattachment point move downstream.

This article is the first of a series of systematic investigation on the wind load characteristics of curve shaped domes in turbulent boundary layer flow and smooth flow. The present investigation focuses on the Reynolds number effects on pressure distribution and the wind load pattern of hemispherical dome in smooth and turbulent boundary layer flows.

2 EXPERIMENT DESIGN

The majority of the wind tunnel tests were conducted in a boundary layer wind tunnel with a 24m(length)×4m(width)×2.6m(height) test section. Both smooth flow and turbulent boundary layer were used. Base plate elevated from floor was used in the case of smooth flow to avoid the boundary layer developed over tunnel floor. The turbulent boundary layer has the characteristics of suburban flow field with power law index α=0.27 and turbulence intensity varies from 25% to 18% in the region of the model heights. Three acrylic hemispherical pressure models with diameters of 120 cm, 50 cm, and 20 cm, designated by Dome L, M, and S, were used in the investigation; the corresponding Reynolds number varies from 5.3×10^4 to 2.0×10^6. Pressure taps were installed along the meridian and three layers of the latitude on the 120cm and 50 cm models; whereas over 200 pressure taps distributed on 8 levels of concentric circles were installed on the 20 cm model to investigate the pressure pattern in different testing conditions. Instantaneous wind pressures were sampled simultaneously at sampling

frequency of 300 Hz, through ZOC pressure scanner system. The blockage ratios of the tests were 0.0015 for Dome S to 0.054 for Dome L. Besides the adjustable ceiling, no further correction for blockage effect was taken. The wind tunnel testing cases are listed in Table 1.

Table.1 Wind tunnel testing conditions

Reynolds number	Diameter	Smooth flow	Boundary layer flow
Dome S	20cm	$6.6 \cdot 10^4$ - $3.4 \cdot 10^5$	$5.3 \cdot 10^4$ - $2.0 \cdot 10^5$
Dome M	50 cm	$1.6 \cdot 10^5$ - $8.7 \cdot 10^5$	$2.0 \cdot 10^5$ - $6.0 \cdot 10^5$
Dome L	120 cm	$5.3 \cdot 10^5$ - $2.0 \cdot 10^6$	$5.8 \cdot 10^5$ - $1.7 \cdot 10^6$

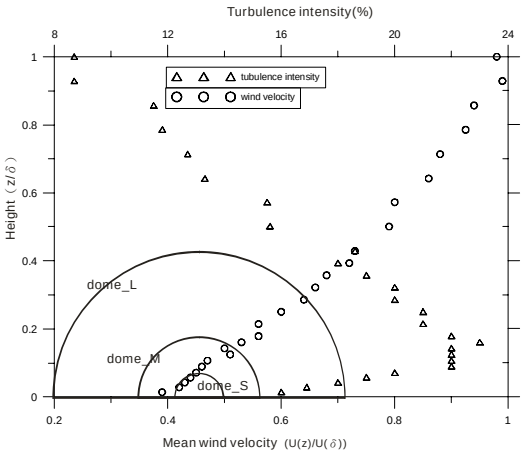

Fig.1 Wind velocity and turbulence intensity profiles (comparing with dome models).

3 DISSCUSSION

3.1 Pressure distribution in smooth flow

The distributions of mean and RMS pressure coefficients along the center meridian at various Reynolds number in smooth flow condition is shown in Figure 2(a) and 2(b). As shown in Figure 2(a), for Reynolds number between 6.7×10^4 ~2.5×10^5, the negative pressure at dome apex increases with Reynolds number, whereas the negative pressure in the wake region decreases. However, for Reynolds number between 3.3×10^5 ~2.0×10^6, the wake suction increases with Reynolds number and the point of separation moves up about 10° upstream. The significant discrepancy of RMS pressure in the front stagnation zone shown in Figure 2(b) is partially due to the effect of thin boundary layer flow developed over base plate onto different size models. This effect of model dimension diminished a θ> 45°. For Re<2.0×10^5 , there are two peaks of C_p' locate at 80°~90°and 110°~120°, suggesting the separation and reattachment; for Re>3.3×10^5, there is only a single peak of C_p' at 110° ~120° 。

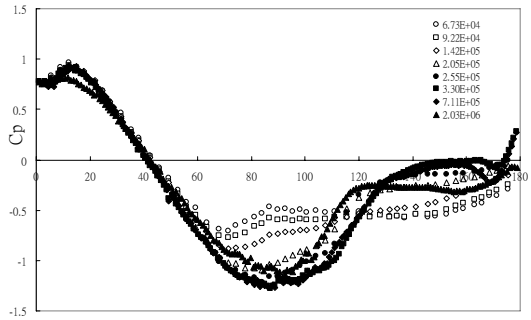

Fig. 2(a) Mean pressure distribution in smooth flow.

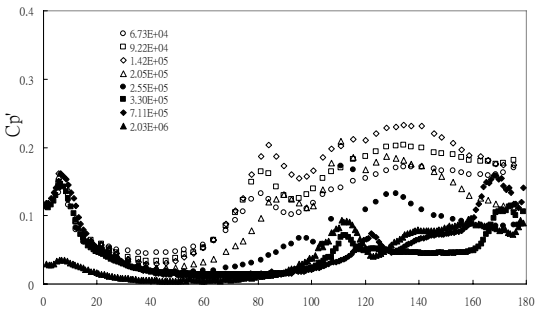

Fig. 2(b) RMS pressure distribution in smooth flow.

The meridian drag coefficients are shown in Figure 3(a) & 3(b). Figure 3(a) indicates that, for Re<3.0×10^5, the mean drag coefficient decreases with the increase of the Reynolds number, and it recovers gradually thereafter. Shown in Figure 3(b), the maximum RMS drag coefficient occurs at $\mathrm{Re} \approx 1.5 \times 10^5$, then decreases rapidly and exhibits a minimum value at $\mathrm{Re} \approx 3.0\times10^5$.

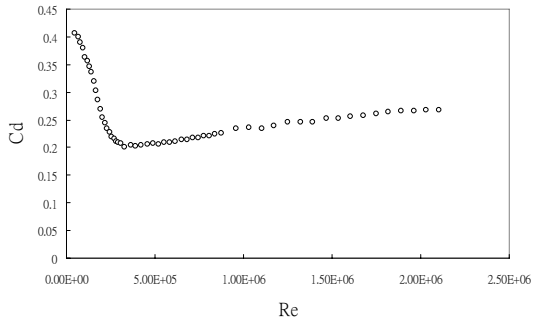

Fig. 3(a) Mean drag coefficient in smooth flow.

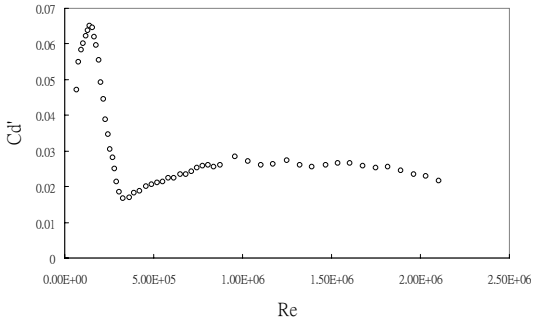

Fig. 3(b) RMS drag coefficient in smooth flow.

3.2 Pressure distribution in turbulent boundary layer flow

Shown in Figure 4(a) and 4(b) are the mean and RMS pressure coefficients along the meridian at various Reynolds number in turbulent boundary layer flow. As shown in Figure 4(a), for Reynolds number between 5.3×10^4 ~1.58×10^5, the negative pressure at dome apex increases, and decreases in wake region. For Reynolds number greater than 1.58×10^5, both the negative pressure at apex and in the wake region show only minor change with respect to Reynolds number. The RMS pressure distribution shown in Figure 4(b) is strongly influenced by the difference of incident turbulence at different height. The RMS pressure exhibits a local

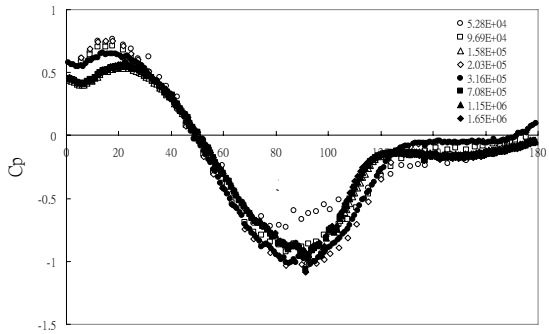

Fig .4(a) Mean pressure distribution in turbulent boundary layer.

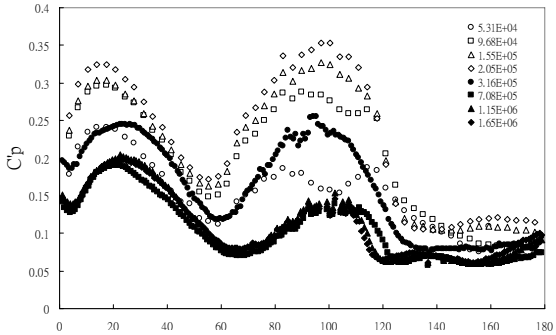

Fig. 4(b) RMS pressure distribution in turbulent boundary layer.

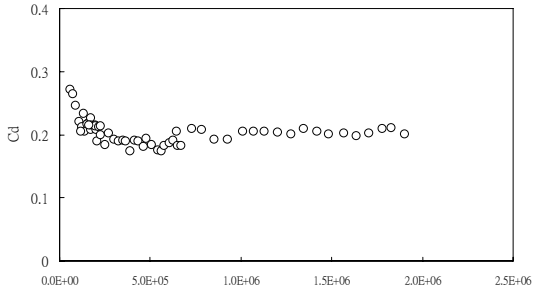

Fig. 5(a) Mean drag coefficient in turbulent boundary layer.

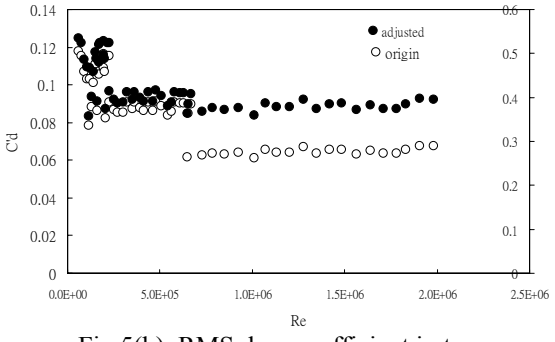

Fig.5(b) RMS drag coefficient in turbulent boundary layer.

peak at the front stagnation zone, at 15°~20°; as for the RMS pressure coefficient in the negative pressure zone: when Re<9.7×10^4, there are two peaks of C_p' locate at 80°~90°and 110°~120°; for Re>1.6×10^5, there is only a single peak of C_p' near 90°~100°. Pressure data suggest that transition of the separation flow occurs at lower Reynolds number in the turbu-

lent boundary layer than the smooth flow. Carefully comparing all pressure measurements of the three different size models, it is concluded that, when Reynolds number is in between $1.5\sim2.0\times10^5$, both C_P and C'_P approach the state of Reynolds number independent.

Shown in Figure 5(a) & 5(b) are the meridian drag coefficients of the domes tested in turbulent boundary layer flow. For $Re<2\times10^5$, The mean drag coefficient decreases with the increase of the Reynolds number; for $Re>2\times10^5$, the mean drag coefficient remains nearly invariant. The open circle symbols in Figure 5(b) represent the original RMS drag coefficients obtained from three dome models. The discrepancies are mostly due to the fact that the incident turbulence intensity levels are not constant at different height in a boundary layer flow as shown in Figure 1. The solid circle symbol represents the RMS drag coefficient further normalized with respect to the turbulence intensity at the dome height, $\tilde{C}_P = C'_P / I_u$, where I_u is the turbulence intensity at dome height. It is noted that the possible effects of different turbulence level can not be eliminated this way. However, after adjustment for turbulence intensity differences, the RMS drag coefficients are in much better agreement, and the data suggest that the RMS drag coefficient becomes invariant when Reynolds number greater than 1.8×10^5.

The Proper Orthogonal Decomposition (POD) was applied to the pressure measurements of Dome S to study the wind load patterns of the hemisphere dome in both smooth and turbulent boundary layer flows. It shows significant differences of wind load patterns between the two flow conditions, the results will be discussed in full paper.

4 CONCLUSIONS

A few concluding remarks can be made based on this investigation:

1. In smooth flow, the transition of separation flow occurs near $Re\approx2.7\times10^5$; the transition occurs at lower Reynolds number, $Re=9.7\times10^4\sim1.5\times10^5$ in the turbulent flow.
2. For hemispherical dome submerged in a suburban type turbulent boundary layer flow, both mean and RMS pressure distributions approach Reynolds number independent when $Re=1.5\sim2.0\times10^5$.
3. In smooth flow, mean drag coefficient decreases with Reynolds number for $Re<3.0\times10^5$, and then increase monotonically up to $Re=2.0\times10^6$; RMS drag coefficient shows maximum and minimum values at $Re\approx1.5\times10^5$ and $Re\approx3.0\times10^5$, respectively. In turbulent boundary layer flow, C_D and C'_D become invariant when $Re>2\times10^5$.

REFERENCES

[1] F.J. Maher, Wind loads on basic dome shapes, J. Struct. Div. ASCE ST3 (1965) 219-228.

[2] T.J. Taylor, Wind pressures on a hemispherical dome, J. Wind Eng. Ind. Aerodyn. 40 (1991) 199-213.

[3] T. Ogawa, M. Nakayama, S. Murayama, Y. Sasaki, Characteristics of wind pressures on basic structures with curved surfaces and their response in turbulent flow, J. Wind Eng. Ind. Aerodyn. 38 (1991) 427-438.

[4] N. Toy, W.D. Moss, E. Savory, Wind tunnel studies on a dome in turbulent boundary layers, J. Wind Eng. Ind. Aerodyn. 1 (1983) 201-212.